Proceedings of the 3rd Croatian Conference on Earthquake Engineering - 3CroCEE
19–22 March 2025, Split, Croatia
Copyright © 2025 CroCEE
DOI: https://doi.org/10.5592/CO/3CroCEE.2025.26

INVESTIGATING THE SEISMIC PERFORMANCE OF THE HONEYCOMB YIELDING DAMPER(HYD)

Zeinolabedin Mortezaali [(1)], Peyman Shadman Heidari [(2)*], Mohammad Ghanooni Bagha [(3)]

(1) Department of Civil Engineering, East Tehran Branch, Islamic Azad University, Tehran, Iran, zizomortezaali@yahoo.com
(2) Department of Civil Engineering, East Tehran Branch, Islamic Azad University, Tehran, Iran, peyman.shademan@iau.ac.ir
(3) Department of Civil Engineering, East Tehran Branch, Islamic Azad University, Tehran, Iran,mohammad_ghanooni@yahoo.com

Abstract

Today, the use of energy-dissipating system such as yielding metal damper in structures can improve the seismic performance of structures. One of the characteristics of metal yielding dampers is the ability to dissipate high energy and increase the ductility of the structural system, which can improve the ductility and energy absorption characteristics of the metal frame equipped with braces and prevent the brace from buckling during an earthquake. The purpose of this research is introduce a new form of yielding dampers called honeycomb yielding damper (HYD) in 28 numerical models with different dimensions and thickness along with evaluating and comparing the force-displacement diagrams and investigating the seismic parameters of this type of yielding damper. All modeling and validation of numerical samples were done by Ansys software. Non-linear analysis method is used in this research. The hysteresis curves are obtained under in-plane cyclic loads. The mechanical parameters such as ductility ratio, initial hardness, effective hardness and damping coefficient can be determin. The results of this research showed that, the effective stiffness increases with the increase in the length of the sample and the Ductility ratio and damping of the equivalent viscous damping. Also, as the thickness of the sample increases, the effective stiffness, the Ductility ratio and the equivalent viscous damping also increases. As the height of the sample increases, the effective stiffness decreases, and the Ductility ratio, the equivalent viscous damping have increased.

Keywords: Yielding honeycomb damper, Ductility ratio, Initial stiffness, Effective stiffness, Equivalent viscous damping.

1. Introduction

Earthquakes are the natural disasters that have occurred in recent years around the world, causing human and financial losses. damping systems are the most popular energy dissipation tools and are used in most projects. These instruments can a large amount of incoming earthquake energy with a predictable performance. In general, seismic control systems are divided into two categories, active control and passive control. Therefore, the use of passive control seismic design methods, such as yielding metal dampers that have the ability to dissipate the incoming energy of earthquake to structures, can improve the seismic performance of structures. The performance of metal dampers based on their non-linear behavior is one of the most effective mechanisms of damping and absorption of energy input to the structure during an earthquake. Kelly et al [1] used the idea of metallic dampers to absorb earthquakes energy in the structure. They introduced several hysteretic energy absorption mechanisms in structures. Skinner et al [2, 3] proposed several yielding metal dampers, including torsion beam dampers, bending beam dampers, and U-shaped dampers. Kasai and Popov [4] presented yielding damper using steel plate and stiffener. They tested it and introduced the hysteresis curve. Bergman and Goel [5] proposed flexural yielding metallic dampers. They tested added damping and stiffness (ADAS) and Triangular-ADAS (TADAS) systems. In ADAS and TADAS dampers are used parallel X and V shaped steel plates, respectively. Whittaker et al [6] tested X-shaped metallic dampers as ADAS under cyclic load. Tsai et al [7], in order to fix the defects of the XADAS dampers, studied TADAS triangular steel plate dampers. Also, they developed a simple mathematical model for force-displacement, which was reasonably accurate compared to laboratory

DOI: https://doi.org/10.5592/CO/3CroCEE.2025.26

work. Dargush and Soong [8] conducted a more detailed study of the phenomenon of fatigue in low cycles based on the behavioral theories of TADAS dampers and developed their analytical models. Gang Li and Hongnan Li [9] presented a new idea for designing metallic damper. They tested dual functions metallic damper (DFMD) with quasi-static loading. Soni and Sanghvi [10] described a technique to find out combined stiffness of model equipped with ADAS damper. They proposed a mathematical model. Teruna et al [11] investigated four steel damper specimens with specific geometry. They obtained energy absorption capabilities, hysteresis loop and stiffness in specimens. Sahoo et al [12] investigated passive energy dissipation of steel plates in both flexure and shear yielding under cyclic loading. Their specimens consist of two flexure (end) plates of X-shape and a shear (web) plate of rectangular shape. Garivani et al [13] introduced a new type of flexural yielding metallic damper and they called comb-teeth damper (CTD). Their damper included number of teeth steel plates that absorb energy through in-plane flexural yielding. Ghaedi et al [14] introduced a new hysteretic metallic bar damper that they named bar damper (BD). BD included three simple steel plates and a number of solid bars which dissipate input energy due to vibration loads through flexural yielding. Kiani [15] designed a model of yielding damper with the hip, chevron, gate, diagonal and knee braces, whose performance reduced the base shear of the system. Moghadisi and Namazi [16] regarding the design of three earthquake-resistant systems, including a structure with a damper, a structure without a damper, and a structure with a chevron brace, which showed that the base shear in a structure with a yield damper is reduced compared to other structures. They also showed that the performance of the structure with yielding damper is better during earthquakes. Yang et al [17] investigated the experimental results of the new HSF honeycomb structure, which shows that the use of the proposed HSF honeycomb structure can provide stable energy dissipation capability as an efficient metal damper for earthquake parameters. Yang et al [18] in a detailed experimental study on the new metal WWFF damper in order to investigate the effect of design parameters such as aspect ratio and slenderness on structural response such as yield strength and stiffness showed that this damper has a stable energy dissipation capacity and can It can be used as an efficient and strong metal damper. Peyman Shadman Heidari [19] presented a new type of metal shear yielding damper in which a perforated shear plate is used and by changing the location and diameter of the holes in DPMD dampers, he investigated the mechanical characteristics of different samples of DPMD dampers.

The purpose of this research is introduce the new form of yielding dampers with different geometry under the name of honeycomb yielding dampers (HYD) with different dimensions and thicknesses. In this reaserch determines their mechanical and seismic characteristics of samples were investigated with the hysteresis curves of the honeycomb yielding damper samples under in-plane cyclic load can determined mechanical parameters such as ductility ratio, initial stiffness, effective stiffness, total dissipated energy, dissipated energy in the last cycle, elastic strain energy, equivalent viscous damping (EVD) and equivalent plastic strain (EPS).

2. Honeycomb yielding damper (HYD)

2.1. Geometry of Honeycomb damper

ADAS dampers are usually used in steel bracing frames, as shown in Figure 1. The HYD dampers can create by drilling a hexagonal shape on a metal sheet and use in metal frame with a chevron brace as shown in Figure 1.

Proceedings of the 3rd Croatian Conference on Earthquake Engineering - 3CroCEE
19–22 March 2025, Split, Croatia

DOI: https://doi.org/10.5592/CO/3CroCEE.2025.26

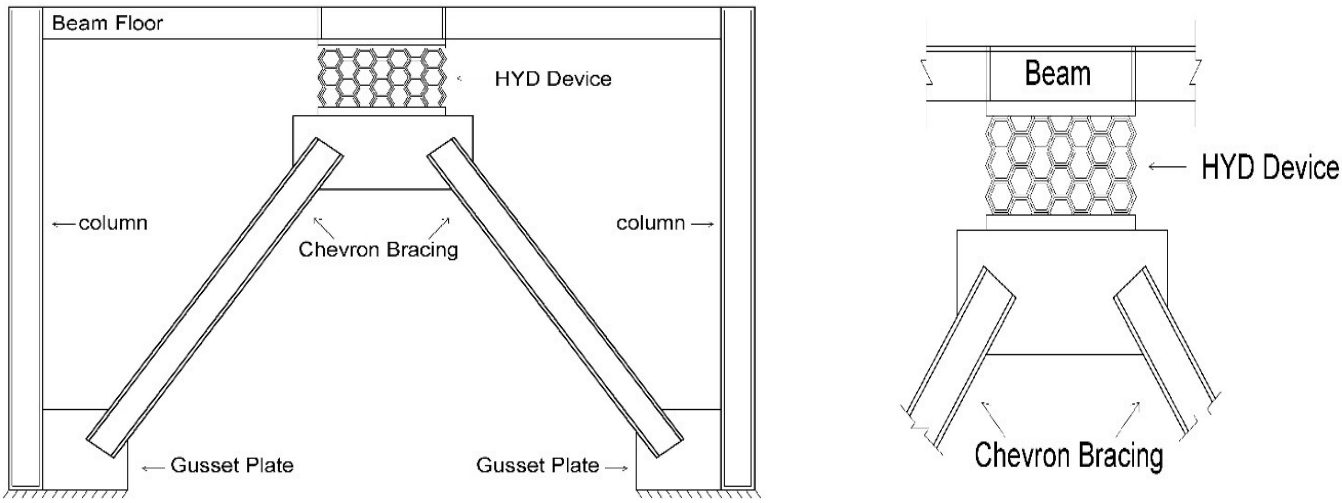

(a) (b)

Figure 1. a) Frame system and HYD position, b) Connection of HYD to beam and bracing

In this research, 28 numerical models are proposed based on different thickness, length and height. The thickness of all samples was considered as 0.48, 0.72, 0.96 and 1.44 cm, respectively. The length of all samples are 41.80, 52.96, 64.12 and 75.28 cm, respectively. Also, samples were considered with different heights of 20.32, 26.76, 33.20 and 39.65 cm. The length of each side of the hexagon is 2.5423 cm and the angle between the sides is 120 degrees. Figure 2 shows the modeling of the honeycomb damper with different lengths, heights and thicknesses. Table 1 shows the specifications and dimensions of the HYD dampers. The Table 1 shows specifications and different dimensions of HYD dampers.

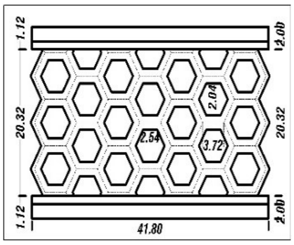

HYD-1-1-1-2

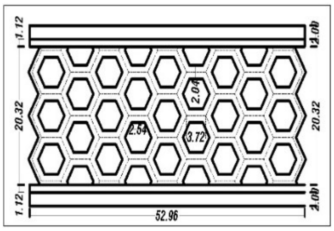

HYD-1-2-1-2

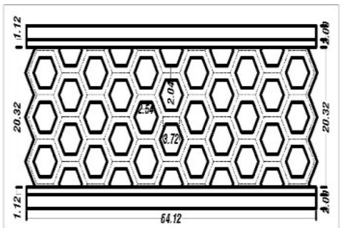

HYD-1-3-1-2

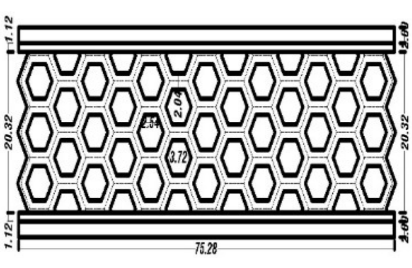

HYD-1-4-1-2

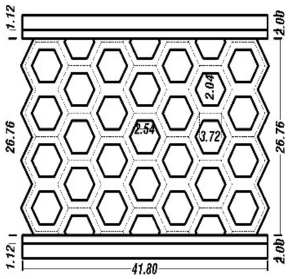

HYD-1-1-2-2

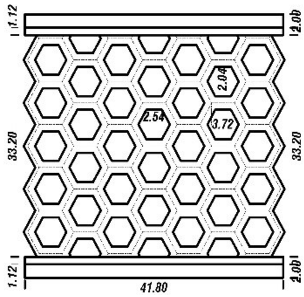

HYD-1-1-3-2

DOI: https://doi.org/10.5592/CO/3CroCEE.2025.26

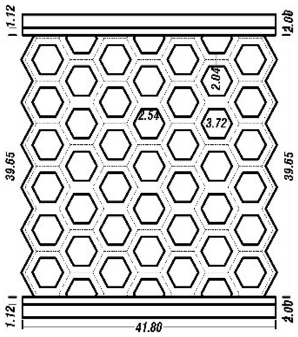

HYD-1-1-4-2

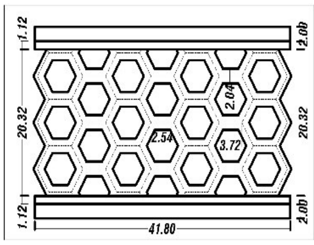

HYD-2-1-1-2

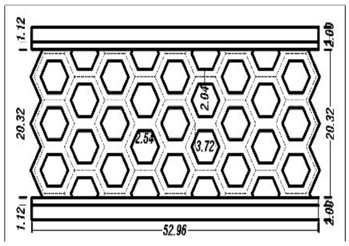

HYD-2-2-1-2

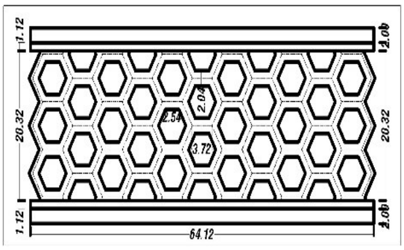

HYD-2-3-1-2

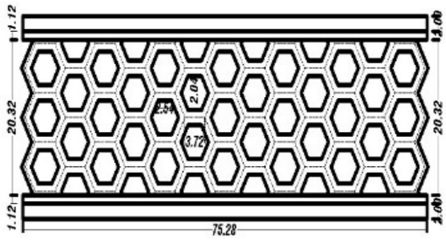

HYD-2-4-1-2

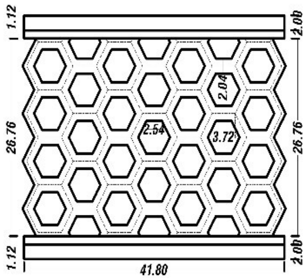

HYD-2-1-2-2

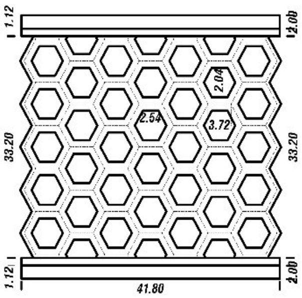

HYD-2-1-3-2

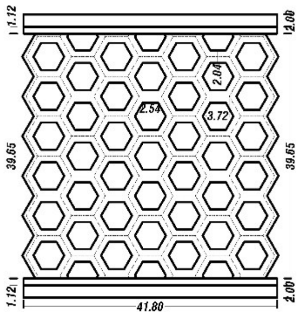

HYD-2-1-4-2

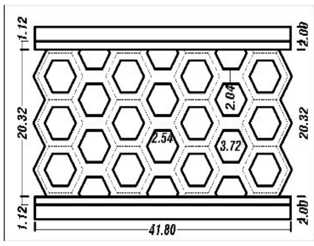

HYD-3-1-1-2

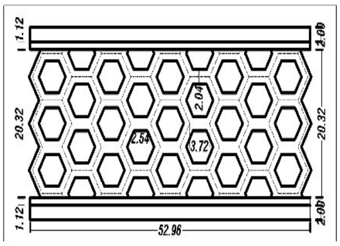

HYD-3-2-1-2

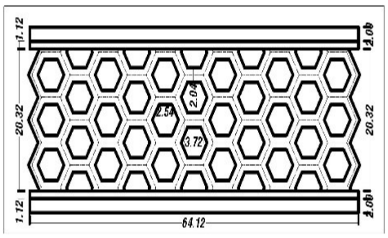

HYD-3-3-1-2

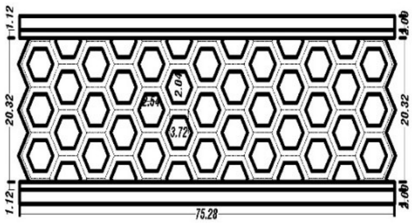

HYD-3-4-1-2

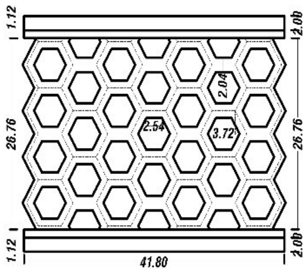

HYD-3-1-2-2

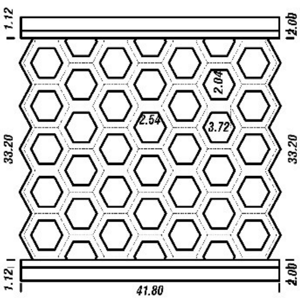

HYD-3-1-3-2

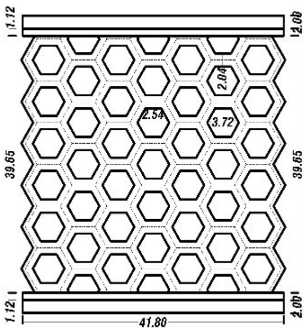

HYD-3-1-4-2

DOI: https://doi.org/10.5592/CO/3CroCEE.2025.26

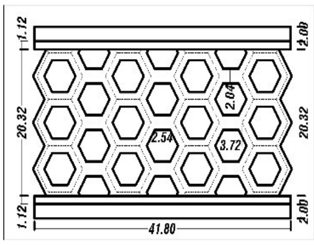

HYD-4-1-1-2

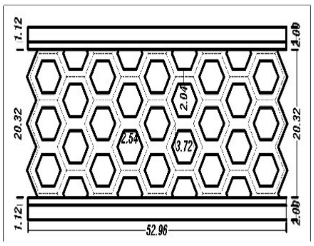

HYD-4-2-1-2

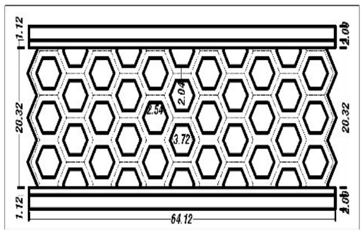

HYD-4-3-1-2

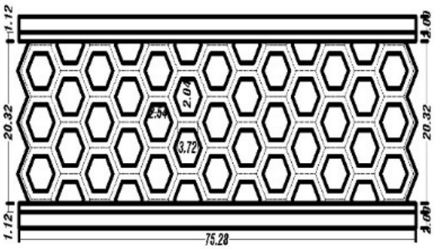

HYD-4-4-1-2

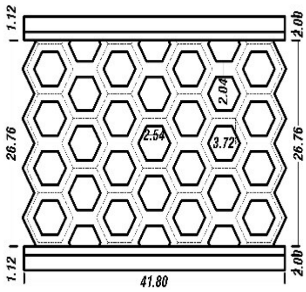

HYD-4-1-2-2

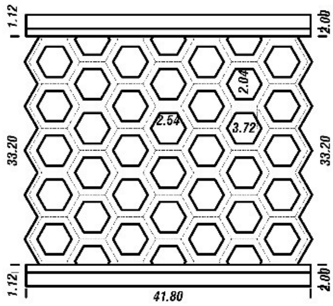

HYD-4-1-3-2

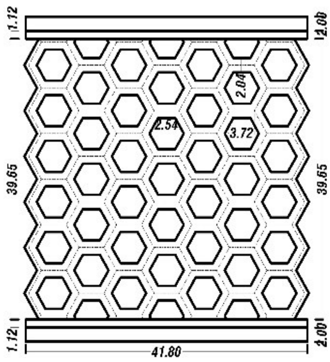

HYD-4-1-4-2

Figure.2. HYD damper modeling with different lengths, heights and thicknesses.

Table 1. Specifications and different dimensions of HYD dampers

Number	Sample	thickness t_p (cm)	Length L(cm)	Hight H(cm)	Length of the hexagon h(cm)
1	HYD-1-1-1-2	0.48	41.80	20.32	2.5423
2	HYD-1-2-1-2	0.48	52.96	20.32	2.5423
3	HYD-1-3-1-2	0.48	64.12	20.32	2.5423
4	HYD-1-4-1-2	0.48	75.28	20.32	2.5423
5	HYD-1-1-2-2	0.48	41.80	26.76	2.5423
6	HYD-1-1-3-2	0.48	41.80	33.20	2.5423
7	HYD-1-1-4-2	0.48	41.80	39.65	2.5423
8	HYD-2-1-1-2	0.72	41.80	20.32	2.5423
9	HYD-2-2-1-2	0.72	52.96	20.32	2.5423
10	HYD-2-3-1-2	0.72	64.12	20.32	2.5423
11	HYD-2-4-1-2	0.72	75.28	20.32	2.5423
12	HYD-2-1-2-2	0.72	41.80	26.76	2.5423
13	HYD-2-1-3-2	0.72	41.80	33.20	2.5423
14	HYD-2-1-4-2	0.72	41.80	39.65	2.5423
15	HYD-3-1-1-2	0.96	41.80	20.32	2.5423
16	HYD-3-2-1-2	0.96	52.96	20.32	2.5423
17	HYD-3-3-1-2	0.96	64.12	20.32	2.5423

DOI: https://doi.org/10.5592/CO/3CroCEE.2025.26

18	HYD-3-4-1-2	0.96	75.28	20.32	2.5423
19	HYD-3-1-2-2	0.96	41.80	26.76	2.5423
20	HYD-3-1-3-2	0.96	41.80	33.20	2.5423
21	HYD-3-1-4-2	0.96	41.80	39.65	2.5423
22	HYD-4-1-1-2	1.44	41.80	20.32	2.5423
23	HYD-4-2-1-2	1.44	52.96	20.32	2.5423
24	HYD-4-3-1-2	1.44	64.12	20.32	2.5423
25	HYD-4-4-1-2	1.44	75.28	20.32	2.5423
26	HYD-4-1-2-2	1.44	41.80	26.76	2.5423
27	HYD-4-1-3-2	1.44	41.80	33.20	2.5423
28	HYD-4-1-4-2	1.44	41.80	39.65	2.5423

2.2. Loading pattern and material properties

In order to evaluate the performance of honeycomb yielding dampers was used AISC 341-16[20] cyclic loading pattern. The relative deformation between the upper and lower plates of the damper is equal to 0.00375 radians for steps 1 to 12 in 6 cycles. for steps 13 to 24 for 6 cycles, the relative deformation between the upper and lower plates of the damper is equal to 0.005 radians for steps 25 to 36 in 6 cycles, the relative deformation is equal to 0.0075 radians for steps 37 to 44 in 4 cycles, the relative deformation is equal to 0.01 radians for steps 45 to 48 in 2 cycles, the relative deformation between the upper and lower plates of the damper is equal to 0.015 radians for steps 49 to 52 in 2 cycles, the relative deformation is equal to 0.02 radians for steps 53 to 56 in 2 cycles, the relative deformation between the upper and lower plates of the damper is equal to 0.03 radians for steps 57 to 60 in 2 cycles, the relative deformation between the upper and lower plates of the damper is equal to 0.04 radians and for steps 61 to 100 in 2 cycles, the relative deformation between the upper and lower plates of the damper is equal to 0.01 radians according to Figure 3-a. In this research, materials with the characteristics of the stress-strain curve used according to Figure 3-b.

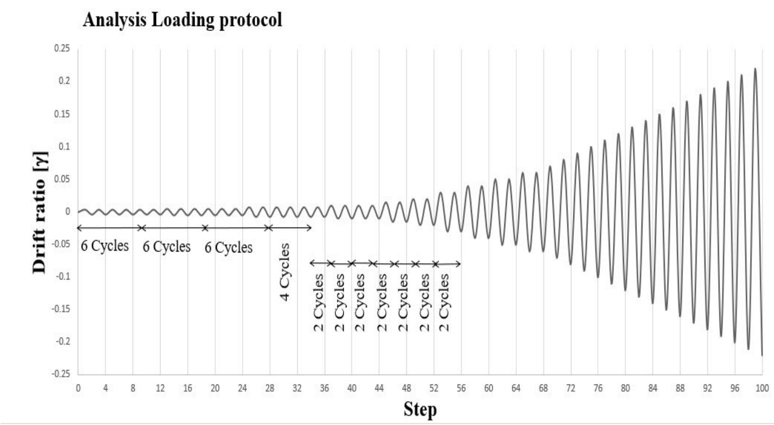

(a)

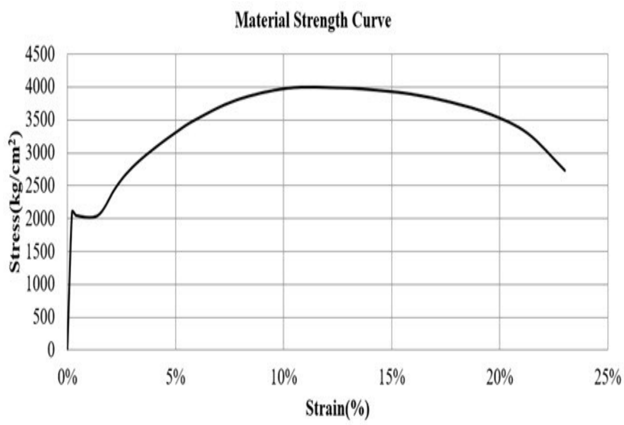

(b)

Figure 3. a) AISC 341-16[20] cyclic loading pattern, b) Stress-strain curve

3. Finite Element Modeling procedure

3.1. FEMs of HYD

To study the mechanical parameters of the honeycomb metallic damper used nonlinear finite element (FEM) analyses with ANSYS R16 FEM [21] software. The 28 finite element models were modeled with different thickness, length and height. Steel plate elements were modeled using a 3D solid element. SOLID 185 (brick 8 node 185) element was used for modeling of proposed samples. Multilinear kinematic hardening plastic model [21] was used to model the plasticity and cyclic inelastic behavior of steel material, respectively. The transitional degree of freedom in the Z and Y

DOI: https://doi.org/10.5592/CO/3CroCEE.2025.26

directions are closed in order to prevent out of plane buckling of the end plate. Mesh sensitivity analysis was performed to find proper element sizes in the FEMs. Figure 4 shows the FEMs of the HYD-1-1-1-2, HYD-1-2-1-2, HYD-1-3-1-2, HYD-1-4-1-2, HYD-1-1-2-2, HYD-1-1-3-2 and HYD-1-1-4-2.

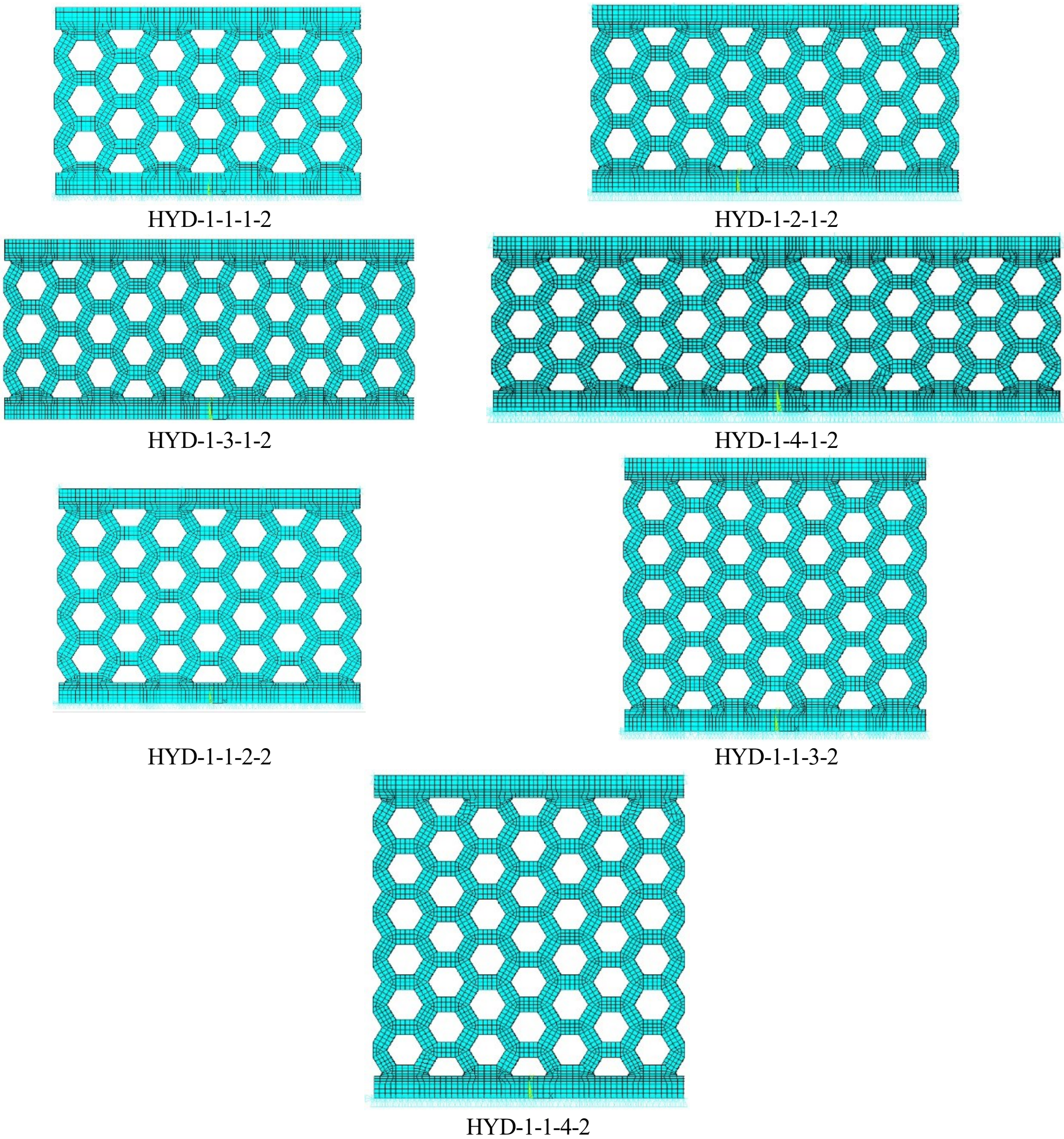

Figure 4. Finite element models of HYD sample

3.2. FEM of HSF experimental specimen

The experimental specimen (HSF [17]) was modeled in ANSYS R16 FEM [21] software in order to validate the FEMs. The displacement ratio applied in the upper sample is γ=10%. The details of the experimental specimen and finite element modeling with ANSYS R16 FEM software [21] show in the Figure 5 respectively.

Proceedings of the 3rd Croatian Conference on Earthquake Engineering - 3CroCEE
19–22 March 2025, Split, Croatia
Copyright © 2025 CroCEE
DOI: https://doi.org/10.5592/CO/3CroCEE.2025.26

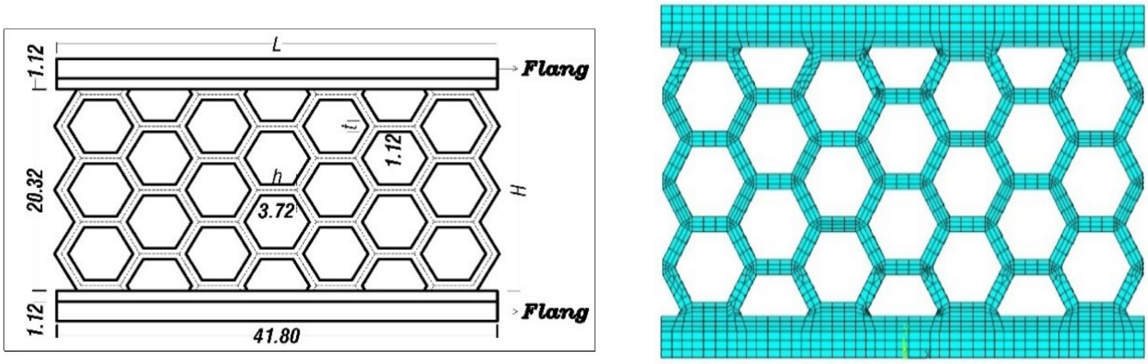

(a) (b)

Figure 5. a) Details of HSF experimental specimen [17], b) Finite element modeling of HSF experimental sample [17]

The results of analytical analysis were compared experimental results. there is an acceptable agreement between the results of analytical and experimental studies according to Figure 6.

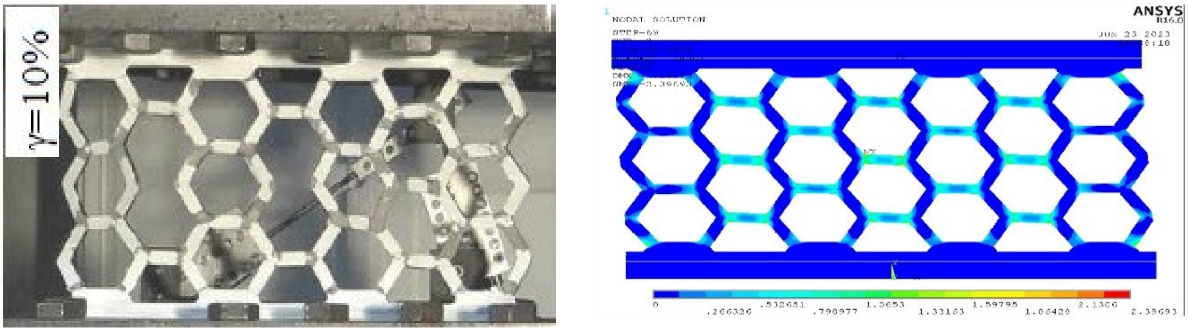

(a) (b)

Figure 6. a) Deformation after loading in HSF experimental specimen [17], b) Deformation after applying loading in the FEM sample with ANSYS R16 FEM[21]

Figure 7 shows the comparison between the hysteresis curves of the HSF experimental specimen [17] and the FEM hysteresis curves.

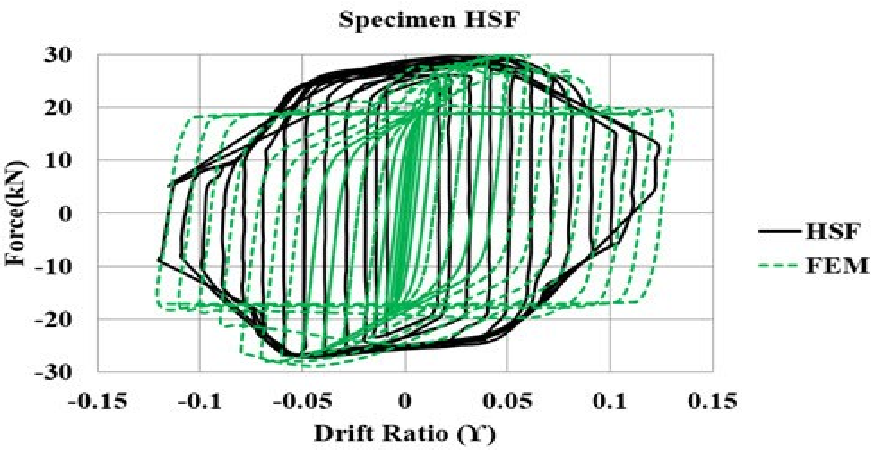

Figure 7. Comparison between the hysteresis curve of the HSF experimental specimen [17] and the FEM sample with ANSYS R16 FEM software [21]

Proceedings of the 3rd Croatian Conference on Earthquake Engineering - 3CroCEE
19–22 March 2025, Split, Croatia

DOI: https://doi.org/10.5592/CO/3CroCEE.2025.26

3.3. Hysteresis behavior of HYDs

Hysteresis curves used to determine the mechanical parameters of the HYD proposed damper. In the force-displacement hysteresis curve can be obtained parameters such as yield force, yield displacement, ultimate force, and ultimate displacement. For this purpose, force-displacement hysteresis curves of analytical samples were determined. Figure 8 shows the force-displacement hysteresis curves of the HYD dampers.

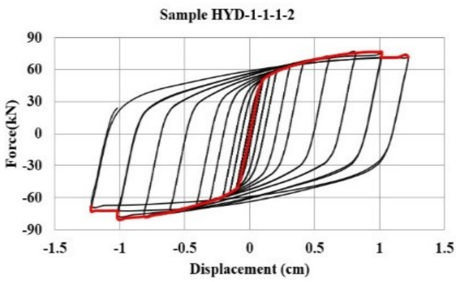

HYD-1-1-1-2

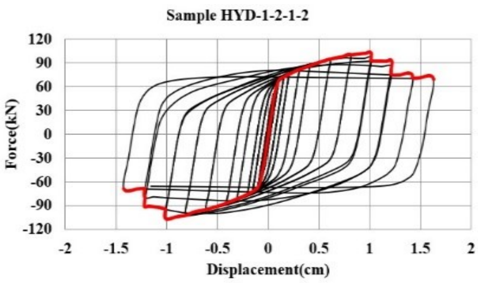

HYD-1-2-1-2

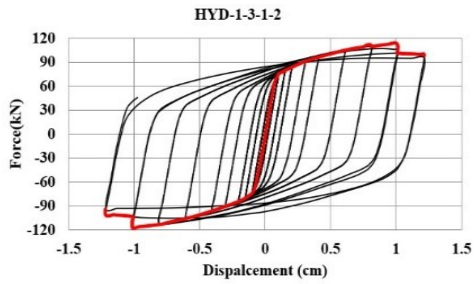

HYD-1-3-1-2

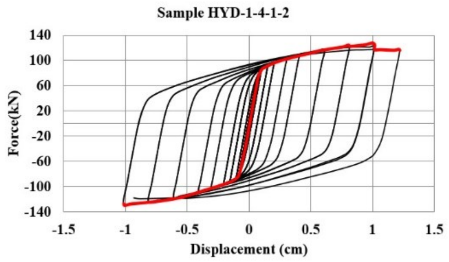

HYD-1-4-1-2

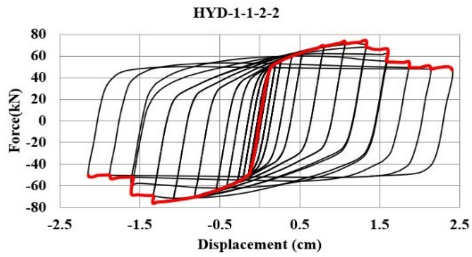

HYD-1-1-2-2

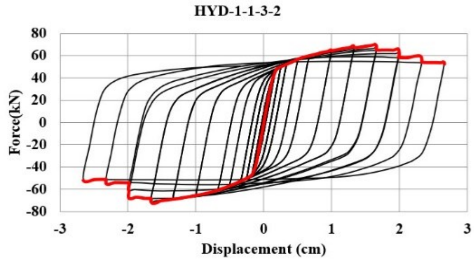

HYD-1-1-3-2

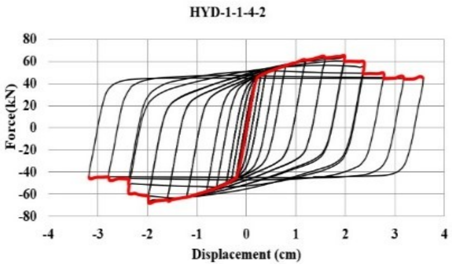

HYD-1-1-4-2

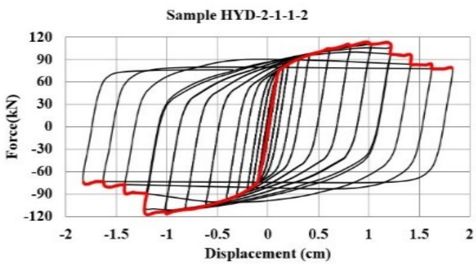

HYD-2-1-1-2

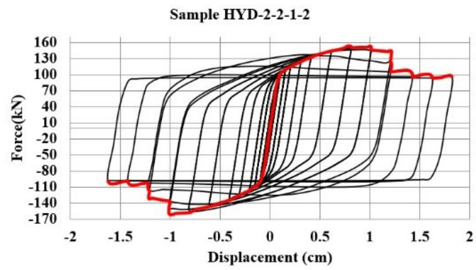

HYD-2-2-1-2

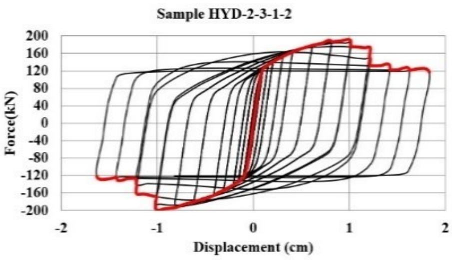

HYD-2-3-1-2

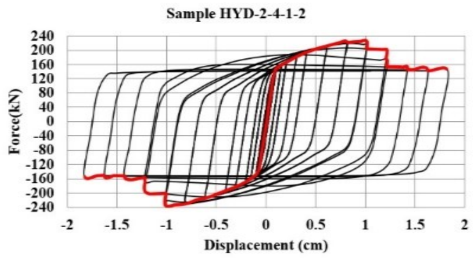

HYD-2-4-1-2

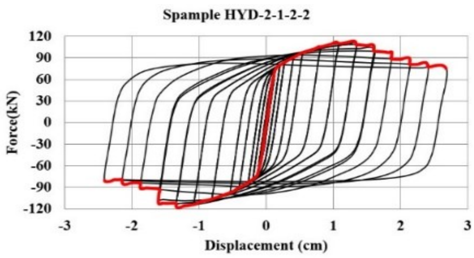

HYD-2-1-2-2

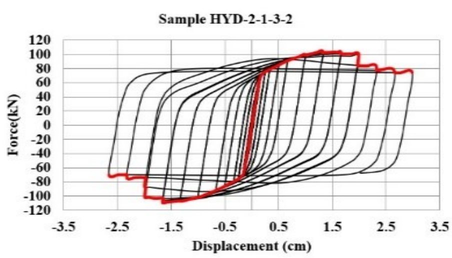

HYD-2-1-3-2

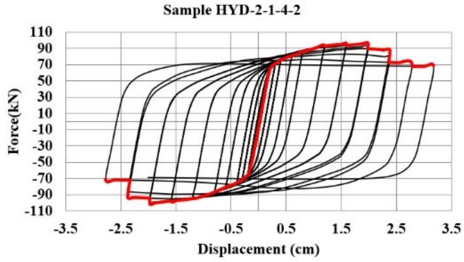

HYD-2-1-4-2

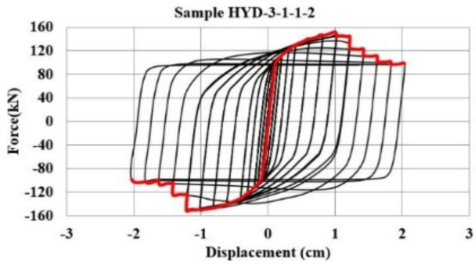

HYD-3-1-1-2

DOI: https://doi.org/10.5592/CO/3CroCEE.2025.26

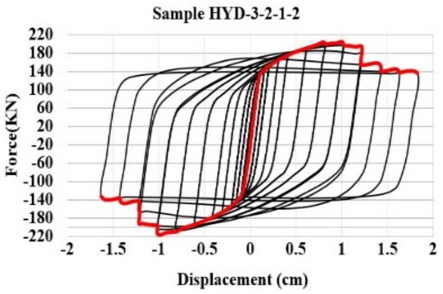

HYD-3-2-1-2

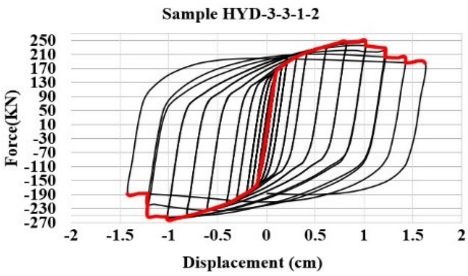

HYD-3-3-1-2

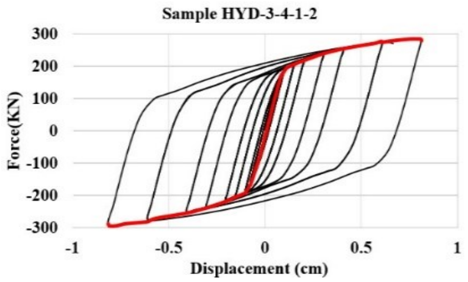

HYD-3-4-1-2

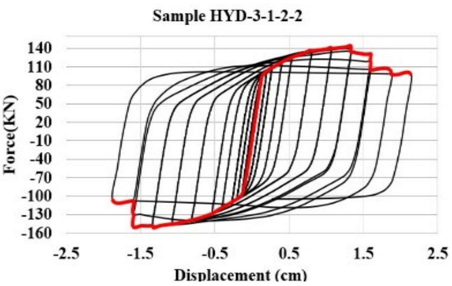

HYD-3-1-2-2

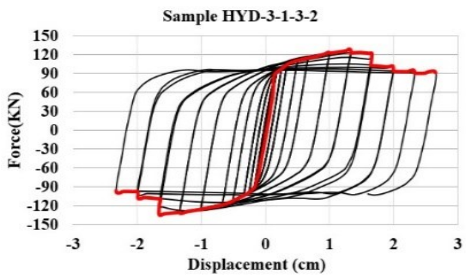

HYD-3-1-3-2

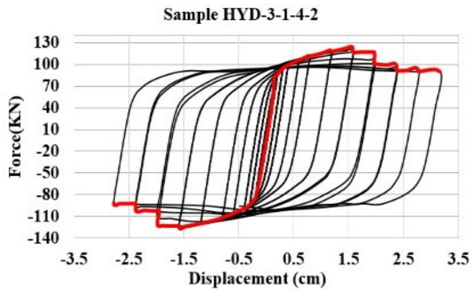

HYD-3-1-4-2

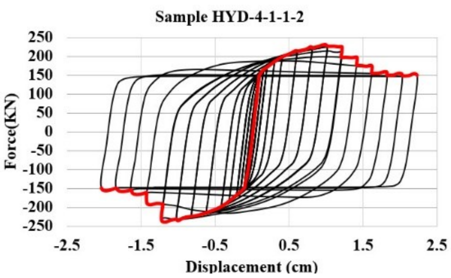

HYD-4-1-1-2

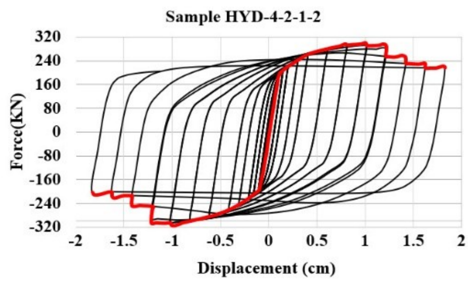

HYD-4-2-1-2

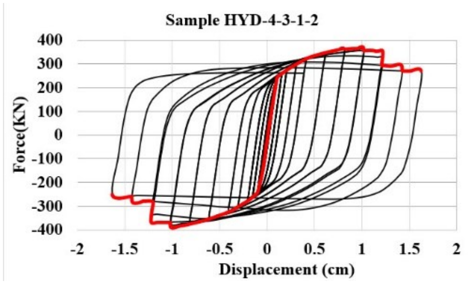

HYD-4-3-1-2

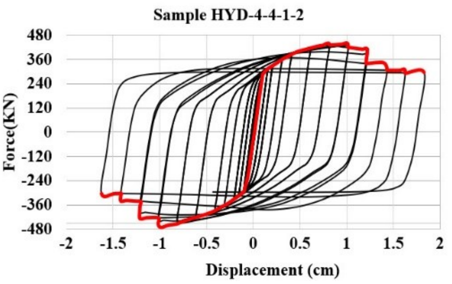

HYD-4-4-1-2

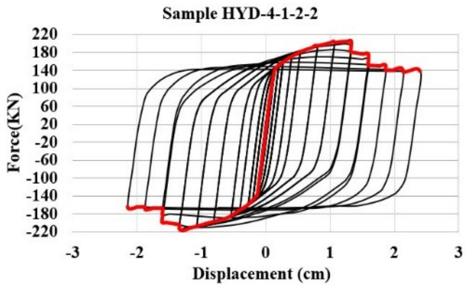

HYD-4-1-2-2

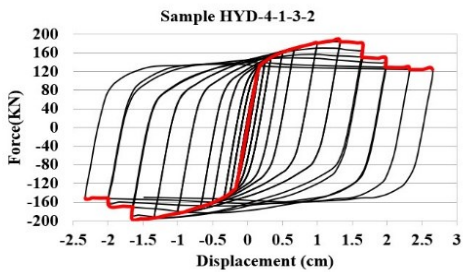

HYD-4-1-3-2

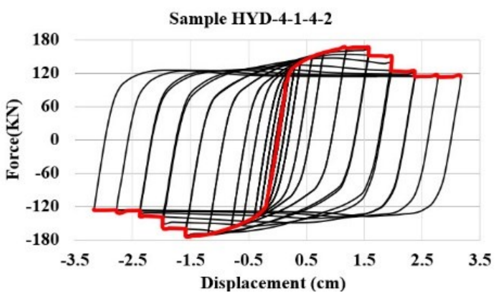

HYD-4-1-4-2

Figure. 8 Force-displacement hysteresis loops of the HYD and backbone curves

DOI: https://doi.org/10.5592/CO/3CroCEE.2025.26

4. Mechanical parameters of HYD dampers

4.1. Ductility ratio, effective and initial stiffness

Ductility ratio can be defined as the ratio of maximum deformation capacity to the deformation level corresponding to a yield deformation. The value of ductility ratio is given by:

$$\mu = \frac{\Delta_{max}}{\Delta_y} \tag{1}$$

Where Δ_{max} and Δ_y are ultimate displacement and yield displacement, respectively. In each loop of the force-deformation hysteresis curve the secant or effective stiffness can be defined. The effective stiffness for maximum displacement was obtained as the average from minimum and maximum force over the average from minimum and maximum displacement, respectively. According to Figure 9, effective stiffness equation is obtained as follows:

$$K_{eff} = \frac{\frac{|P_{max}|+|P_{min}|}{2}}{\frac{|\Delta_{max}|+|\Delta_{min}|}{2}} = \frac{P_{ave}}{\Delta_{ave}} \tag{2}$$

Where Δ_{max} , Δ_{min} , Δ_{ave} , P_{max} , P_{min} and P_{ave} are ultimate displacement, minimum displacement, average displacement, ultimate force, minimum force, average force in each loop, respectively. In this research, effective stiffness was calculated for maximum displacement and last loop of the force displacement hysteresis curves of the HYD samples. Also, initial stiffness is calculated as follows:

$$K_{initial} = \frac{P_y}{\Delta_y} \tag{3}$$

Where Δ_y and P_y are yield displacement and yield force, respectively. In this paper, initial stiffness was calculated for first loop of the force-displacement hysteresis curves of the HYD samples. Effective stiffness represents the damping force in response to the desired displacement. The ultimate displacement and yield displacement values were obtained from the force-displacement hysteresis curve. Table 2 illustrates the ductility ratio, effective stiffness and initial stiffness for the HYD samples. Figure 9 shows the effective stiffness, dissipated energy, and elastic strain energy in the last loop of the hysteresis curve[19]. Figure 10 show the Ductility ratio (μ) and effective stiffness (K_{eff}) of HYD samples.

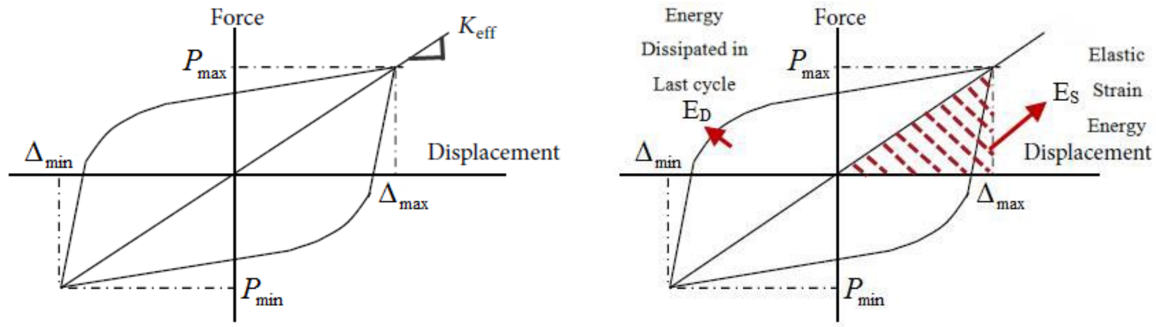

Figure. 9 Effective stiffness, dissipated energy and elastic strain energy in the last loop of the hysteresis curve [19]

Proceedings of the 3[rd] Croatian Conference on Earthquake Engineering - 3CroCEE
19–22 March 2025, Split, Croatia

DOI: https://doi.org/10.5592/CO/3CroCEE.2025.26

Table 2. Ductility ratio, effective stiffness and initial stiffness of HYD samples

Number	Sample	Δ_y (cm)	Δ_{max} (cm)	Δ_{min} (cm)	Δ_{ave} (cm)	P_y (KN)	P_{min} (KN)	P_{max} (KN)	P_{ave} (KN)	μ	k_{inital} (KN/ cm)	k_{eff} (KN/cm)
1	HYD-1-1-1-2	0.109	1.0096	-0.992	1.00	50.53	-80.53	76.96	79	9.26	463.6	78.66
2	HYD-1-2-1-2	0.1066	1.0038	-0.902	0.95	67.80	-104.2	103.7	104	9.41	635.7	109.1
3	HYD-1-3-1-2	0.1049	0.9992	-1.009	1.00	75.49	-117.7	114.1	116	9.52	719.5	115.4
4	HYD-1-4-1-2	0.1013	0.9961	-1.004	1.00	86.09	-129.7	127.7	129	9.83	749.5	128.5
5	HYD-1-1-2-2	0.1289	1.3286	-1.314	1.32	47.57	-76.03	74.37	75	10.30	368.9	56.90
6	HYD-1-1-3-2	0.1595	1.6483	-1.637	1.64	44.48	-72.43	69.14	71	10.33	278.9	43.09
7	HYD-1-1-4-2	0.1848	1.9596	-1.959	1.96	40.87	-68.17	65.51	67	10.60	221.1	34.11
8	HYD-2-1-1-2	0.0979	0.9767	-1.193	1.09	69.52	-117.6	113.2	115	9.97	709.8	106.3
9	HYD-2-2-1-2	0.8545	0.8017	-0.970	0.89	94.69	-160.9	153.7	157	9.38	1108.3	177.4
10	HYD-2-3-1-2	0.1055	0.9852	-0.990	0.99	125.3	-199.1	191.3	195	9.33	1187.8	197.5
11	HYD-2-4-1-2	0.1083	1.0023	-0.985	0.99	149.1	-237.0	226.6	232	9.25	1376.0	233.2
12	HYD-2-1-2-2	0.1352	1.3012	-1.312	1.31	72.76	-118.6	112.8	116	9.62	537.80	88.55
13	HYD-2-1-3-2	0.1292	1.3097	-1.626	1.47	60.12	-109.9	105.1	108	10.14	465.30	73.23
14	HYD-2-1-4-2	0.1923	1.9677	-1.954	1.96	62.53	-102.0	96.99	100	10.23	325.0	50.74
15	HYD-3-1-1-2	0.0964	0.9867	-1.205	1.10	93.11	-152.6	151.3	152	10.24	965.80	138.6
16	HYD-3-2-1-2	0.0999	1.0015	-0.977	0.99	129.9	-215.6	204.0	210	10.02	1300.3	212.0
17	HYD-3-3-1-2	0.0983	0.9726	-0.979	0.98	158.7	-263.7	249.8	257	9.89	1614.4	263.1
18	HYD-3-4-1-2	0.0858	0.806	-0.798	0.80	172.7	-295.4	283.2	289	9.40	2012.8	360.5
19	HYD-3-1-2-2	0.1341	1.3223	-1.327	1.33	94.62	-151.0	144.8	148	9.86	705.4	111.6
20	HYD-3-1-3-2	0.1298	1.3121	-1.63	1.47	81.93	-134.8	129.0	132	10.11	631.2	89.68
21	HYD-3-1-4-2	0.1455	1.5487	-1.571	1.56	80.52	-127.6	124.5	126	10.64	553.5	80.81
22	HYD-4-1-1-2	0.0961	0.9923	-1.191	1.09	138.4	-239.7	230.0	235	10.32	1440.2	215.1
23	HYD-4-2-1-2	0.0979	0.9999	-0.975	0.99	182.9	-314.4	300.7	308	10.21	1867	311.3
24	HYD-4-3-1-2	0.1003	1.0032	-0.988	1.00	231.2	-391.3	371.6	381	10.00	2304.6	383.1
25	HYD-4-4-1-2	0.1004	0.9934	-0.993	0.99	283.6	-469.6	440.7	455	9.89	2823.6	458.2
26	HYD-4-1-2-2	0.1325	1.3273	-1.298	1.31	134.3	-216.6	207.2	212	10.01	1013.5	161.4
27	HYD-4-1-3-2	0.1290	1.3048	-1.617	1.46	110.2	-198.3	190.3	194	10.11	853.7	133.0
28	HYD-4-1-4-2	0.1421	1.5486	-1.552	1.55	101.7	-175.3	167.6	171	10.90	715.7	110.5

DOI: https://doi.org/10.5592/CO/3CroCEE.2025.26

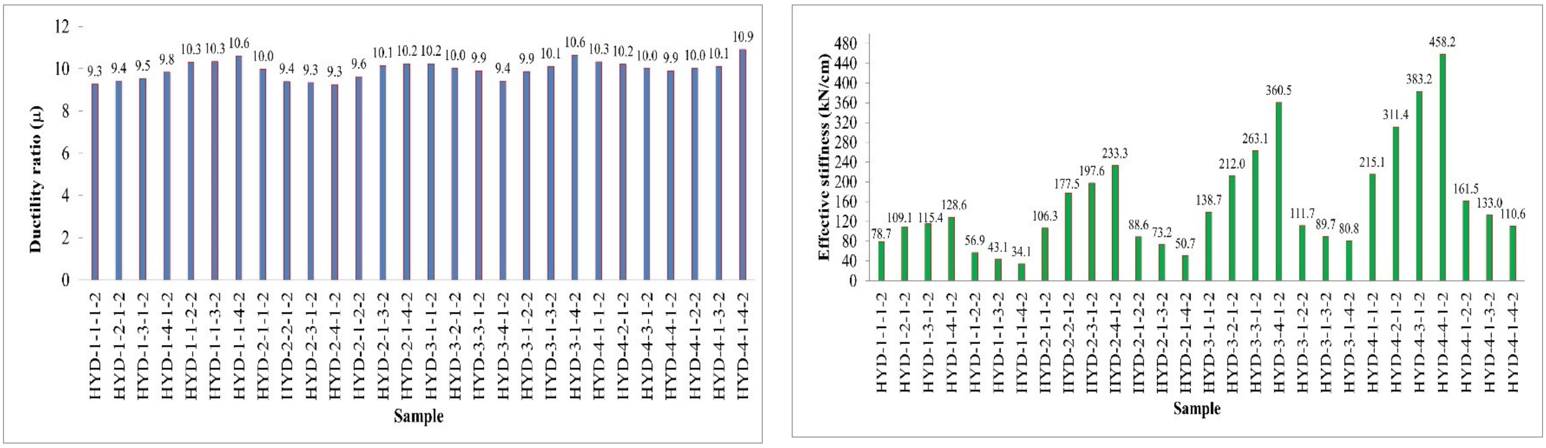

(a) (b)

Figure 10. a) Ductility ratio (μ) of HYD samples, Figure 10. b) Effective stiffness (K_{eff}) of HYD samples.

According to Figure 10-a by increasing the sample length from 41.80 cm to 75.28 cm, the Ductility ratio in HYD samples decreases and by increasing the height from 20.32 cm to 33.20 cm, this ratio increases and by increasing the thickness this ratio increases. In sample HYD-2-1-1-2 with a length of 41.80 cm and a Ductility ratio of 9.97, with an increase in length of 52.96 cm in sample HYD-2-2 1-2- The Ductility ratio decreased to 9.38 and by increasing the length again to 75.28 cm in sample HYD-2-4-1-2, the Ductility ratio was 9.25 it has decreased by 7.49% compared to HYD-2-1-1-2 sample. In the HYD-1-1-1-2 sample with a height of 20.32 cm and a thickness of 0.48 cm and a Ductility ratio of 9.26, with a height increase of 39.65 cm in the HYD-1-1-4-2 sample, the Ductility ratio has increased to 10.60, and the Ductility ratio has increased by 13.49% compared to HYD-1-1-1-2 sample. In sample HYD-1-1-1-2 with a thickness of 0.48 cm, with the increase the thickness in sample HYD-2-1-1-2 by 0.72, the Ductility ratio increased to 9.97 and by increasing the thickness of the sample to 0.96 cm in the HYD-3-1-1-2 sample, the Ductility ratio has increased to 10.24 which increases by 7.38% and 10.05% compared to HYD-1-1-1-2 sample and as a result, due to the increase in the thickness of the samples, it can be expected that the Ductility ratio in the samples will increase.

According to the values obtained from Figure 10-b, HYD-1-1-1-2 sample with a length of 41.80 cm has an effective stiffness of 78.66 KN/cm, which increases to 52.96, 64.12 and 75.28 cm in HYD -1-2-1-2, HYD-1-3-1-2 and HYD-1-4-1-2, samples respectively, amounting to 109.10, 115.44 and 128.57 KN/cm have increased, and the effective stiffness has increased by 32.42%, 37.89%, and 48.16%, respectively, compared to HYD-1-1-1-2 sample. In sample HYD-1-1-1-2 with a height of 20.32 cm, which by increasing the height to 26.76, 33.20 and 39.65 cm in samples HYD-1-1-2-2, HYD-1-1-3-2 and HYD-1-1-4-2 The effective stiffness decreased to 56.90, 43.09 and 34.11 KN/cm, respectively, which compared to HYD-1-1-1-2 sample, respectively, by It has decreased by 32.10%, 58.43% and 79.01%. Regarding the increase in thickness, the effective stiffness of the HYD-1-1-1-2 sample is 78.66 KN/cm, which by increasing the thickness to 1.44 cm in the HYD-4-1-1-2 sample is 215.14 KN/cm increases, which has increased by 92.90%.

4.2. Hysteresis damping coefficient

The equivalent viscous damping (EVD) or effective damping is effective index in evaluating the seismic performance of passive energy dissipation systems. The EVD has defined the combined effects of elastic and hysteretic damping. The EVD concept was first proposed by Jacobsen [17, 18]. The value of EVD based on Jacobsen's approach can be calculated with equation 4. The ξhyst represents the dissipation energy due to the hysteretic behavior.

$$\zeta_{hyst} = \frac{E_D}{4\pi E_S} = \frac{E_D}{2\pi K_{eff}\delta_{ave}{}^2} \tag{4}$$

DOI: https://doi.org/10.5592/CO/3CroCEE.2025.26

Table 3 shows the value of ζhyst for 28 HYD samples for the ultimate displacement.

Table 3. Total dissipated energy (ET), dissipated energy in the last cycle (ED)elastic strain energy (ES) and EVD of HYD samples and proposed formula

Number	**Sample**	E_T (KN.cm)	E_D (KN.cm)	E_S (KN.cm)	$\frac{E_D}{E_T}$	$\frac{E_S}{E_T}$	**ζhyst (%)**
1	HYD-1-1-1-2	1760.40	257.60	39.40	14.60%	2.20%	52.00
2	HYD-1-2-1-2	3062.30	402.20	49.60	13.10%	1.60%	64.20
3	HYD-1-3-1-2	2579.80	356.90	58.20	13.80%	2.30%	48.80
4	HYD-1-4-1-2	2511.20	385.00	64.30	15.30%	2.60%	47.60
5	HYD-1-1-2-2	3214.90	429.30	49.70	13.40%	1.50%	68.70
6	HYD-1-1-3-2	3553.90	496.10	58.10	14.00%	1.60%	67.90
7	HYD-1-1-4-2	4241.40	566.80	65.50	13.40%	1.50%	68.90
8	HYD-2-1-1-2	4058.70	524.20	62.60	12.90%	1.50%	66.60
9	HYD-2-2-1-2	5294.60	633.70	69.70	12.00%	1.30%	72.30
10	HYD-2-3-1-2	6441.50	792.00	96.50	12.30%	1.50%	65.30
11	HYD-2-4-1-2	8244.90	1018.40	115.20	12.40%	1.40%	70.30
12	HYD-2-1-2-2	6032.80	757.20	75.60	12.60%	1.30%	79.70
13	HYD-2-1-3-2	5705.00	770.50	79.00	13.50%	1.40%	77.70
14	HYD-2-1-4-2	5843.90	795.60	97.60	13.60%	1.70%	64.90
15	HYD-3-1-1-2	6330.10	755.20	83.30	11.90%	1.30%	72.20
16	HYD-3-2-1-2	6907.50	893.10	103.80	12.90%	1.50%	68.50
17	HYD-3-3-1-2	7439.80	1067.60	125.30	14.30%	1.70%	67.80
18	HYD-3-4-1-2	2913.90	582.40	116.10	20.00%	4.00%	39.90
19	HYD-3-1-2-2	5644.80	756.80	98.00	13.40%	1.70%	61.40
20	HYD-3-1-3-2	6299.10	885.50	97.00	14.10%	1.50%	72.60
21	HYD-3-1-4-2	7410.60	1027.20	98.40	13.90%	1.30%	83.10
22	HYD-4-1-1-2	10238.80	1202.00	128.20	11.70%	1.30%	74.60
23	HYD-4-2-1-2	10722.50	1436.30	151.90	13.40%	1.40%	75.20
24	HYD-4-3-1-2	11871.20	1618.20	189.90	13.60%	1.60%	67.80
25	HYD-4-4-1-2	15267.10	1969.60	226.10	12.90%	1.50%	69.30
26	HYD-4-1-2-2	9544.10	1277.40	139.10	13.40%	1.50%	73.10
27	HYD-4-1-3-2	9658.90	1309.80	142.00	13.60%	1.50%	73.40
28	HYD-4-1-4-2	11192.40	1467.60	132.90	13.10%	1.20%	87.90

According to table 3, the hysteresis damping of the sample HYD-1-1-1-2 with a thickness of 0.48 cm is 52.00%. Compared to the sample HYD-4-1-1-2 with a thickness of 1.44 cm, this amount has decreased by 74.60%. Therefore, with the increase in the thickness of the sample, the hysteresis damping decreases. Also, by increasing the height of the HYD-1-1-4-2 sample by 39.65 cm, the hysteresis damping increases by 68.90% compared to the HYD-1-1-1-2 sample.

5. Conclusions

In this research, a new type of yielding metal dampers called honeycomb dampers was introduced. According to the analysis, it was found that the effective stiffness increases with the increase in the length of the sample and the Ductility ratio and damping of the equivalent viscous damping. Also, as the thickness of the sample increases, the effective stiffness, the Ductility ratio and the equivalent viscous damping also increases. As the height of the sample increases, the effective stiffness decreases, and the Ductility ratio, the equivalent viscous damping have increased. The highest effective stiffness value related to the HYD-4-4-1-2 sample, which has the longest length and the largest thickness, and its effective stiffness is equal to 121.57 KN/cm. The highest effective stiffness value is related to the HYD-4-4-1-1 sample, which has the longest length and the largest thickness, and its effective stiffness is equal to 458.20 KN/cm which has increased by 141.39% compared to HYD-1-1-1-2 sample. The highest Ductility ratio value is related to the HYD-4-1-4-2 sample, and it has a Ductility ratio to 10.90. In the end, it is suggested that the performance of the honeycomb yielding damper is improved by increasing the length and thickness.

References

[1] Kelly J.M, Skinner R.1, Heine A.J. Mechanisms of Energy Absorption in Special Devices for Use in Earthquake Resistant Structures. Bulletin of N. Z. Society of Earthquake Engineering, Vol. 5 No. 3, 1972.

[2] Skinner R.1, Kelly J.M, Heine A.J. Hysteretic Dampers for Earthquake Resistant Structures. Earthquake Engineering and Structural Dynamics, 287- 296, 1975.

[3] Skinner R.1, Tyler R.G, Heine A.J, Robinson W.H. Hysteretic Dampers for the Protection of Structures from Earthquakes. Bulletin of N. Z. Society of Earthquake Engineering, Vol 13. No 1, 1980.

[4] Kasai K, Popov E.P. General behavior of WF steel shear link beams. J. Struc. Eng, 112(2): 362-382, 1986.

[5] Bergman D. M, Goel S.C. Evaluation of cyclic testing of steel plate device for added damping and stiffness. Report No. UMCE 87-10, the University of Michigan, Ann Arbor, MI, 1987.

[6] Whittaker A.S, Bertero V.V, Thompson C. L, Alonso L.J. Seismic Testing of Steel Plate Energy Dissipation Devices. Earthquake Spectr; 7(4): 563-604, 1991.

[7] Tsai K.C, Chen H.W, Hong C.P, Su Y.F. Design of steel triangular plate energy absorbers for seismic-resistance construction. Earthquake Spectra; 9(3): 505-528, 1993.

[8] Dargush G.F, Soong T.T. Behavior of Metallic Plate Dampers in Seismic Passive Energy Dissipation Systems. Earthquake Spectra; 11(4): 545-568, 1995.

[9] Gang Li, Hongnan Li. Earthquake resistant design of RC frame with dual functions metallic damper. The 14th World Conference on Earthquake Engineering. Beijing, China, 2008.

[10] Soni A.H, Sanghvi C.S. Mathematical modeling of ADAS damper element and nonlinear time history analysis of SDOF steel structure using ETABS. Journal of Engineering Research and Studies, 2012.

[11] Teruna D.R, Majid T.A, Budiono B. Experimental Study of Hysteretic Steel Damper for Energy Dissipation Capacity. Advances in Civil Engineering, Article ID 631726, 12 pages, 2015.

[12] Sahoo D.R, Singhal T, Taraithia S.S, Saini A. Cyclic behavior of shear-and-flexural yielding metallic dampers. Journal of Constructional Steel Research; (114): 247–257, 2015.

[13] Garivani S, Aghakouchak A.A, Shahbeyk S. Numerical and Experimental Study of Comb-Teeth Metallic Yielding Dampers. International Journal of Steel Structures; 16(1): 177-196, 2016.

[14] Ghaedi K, Ibrahim Z, javanmardi A. A new metallic bar damper device for seismic energy dissipation of civil structures. 14th International Conference on Concrete Engineering and Technology, 2018.

[15] Kiai, M. Evaluation of the performance of metal yielding dampers in steel structures, Faculty of Civil Engineering, Noshirvan University of Technology, Babol, 2018.

[16] Moghadasi M, Namazi A. Assessment of pearformance of TADAS dampers for the Seismic rehabilitation of buildings. International Journal of Applied Engineering Research; 11(21): 10516-10523, 2016.

DOI: https://doi.org/10.5592/CO/3CroCEE.2025.26

[17] Yang T.Y, Tianyi Li, Tobber L, Pan X. Experimental Test of Novel Honeycomb Structural Fuse. The 14th Nordic Steel Construction Conference, Copenhagen, Denmark, 451-456, 2019.

[18] Yang T.Y, Banjuradja W, Tobber L. Experimental Test of Welded Wide Flange Fuses. key Engineering Materials; (763): 414-422, 2018.

[19] Shadman Heidari P. numerical study on mechanical parameters of novel drilled plate metallic damper (DPMD). Proceedings of the 2nd Croatian Conference on Earthquake Engineering, 505-516, 2023.

[20] ANSI/AISC 341-16. Seismic provisions for structural steel buldings. An american national standard, 9.1-148, 2016.

[21] ANSYS Meshing User's Guide, (2016), Release 16.0. ANSYS, Inc.

[22] Jacobsen L.S. Steady forced vibration as influenced by damping. Transactions of ASME, 52, 169-181, 1930.

[23] Jacobsen L.S. Damping in composite structures, Proceedings of the Second World Conference on Earthquake Engineering, Vol 2, 1029-1044, (1960).